dual-loop approach, and adequate for an LO source for an LMDS down converter.

REFERENCES

1. D.A. Gray, A broadband wireless access system at 28 GHz, Wireless Commun Conf, Boulder, CO, Aug. 1997, pp. 1–7.
2. A. Nordbtten, LMDS systems and their application, IEEE Commun Mag (June 2000), 150–154.
3. F. Losee, RF systems, components, and circuits handbook, Artech House, Boston, MA, 1997, pp. 163–166.
4. B. Razavi, Challenges in the design of frequency synthesizers for wireless applications, Proc IEEE 1997 Custom Integrated Circuits Conf, Santa Clara, CA, May 1997, pp. 395–402.
5. K. Kamogawa, T. Tokmitsu, and I. Toyoda, A 20-GHz-band subharmonically injection-locked oscillator MMIC with wide locking range, IEEE Microwave Guided Wave Lett 7 (1997), 233–235.
6. S. Kudszus, W.H. Haydl, A. Bangert, R. Osorio, M. Neumann, L. Veweyen, A. Huelsman, and M. Schlechtweg, HEMT oscillator for millimeter-wave systems in coplanar waveguide technology, 28th European Microwave Conf Proc, Amsterdam, The Netherlands, Oct. 1998, vol. 2, pp. 759–765.
7. K. Kamogawa, T. Tokumistsu, and M. Aikawa, Injection-locked oscillator chain: A possible solution to millimeter-wave MMIC synthesizers, IEEE Trans Microwave Theory Tech 45 (1997), 1578–1584.
8. Q. Xue, A subharmonically injection-locked dual-gate FET VCO frequency synthesizer, Microwave Opt Technol Lett 26 (2000).
9. K. Kurokawa, Injection locking of microwave solid-state oscillators, Proc IEEE 61 (1973), 1386–1410.

NONDESTRUCTIVE DETERMINATION OF THE LONGITUDINAL CHROMATIC DISPERSION DISTRIBUTION ALONG AN OPTICAL FIBER

P. K. A. Wai,[1] F. Moldoveanu,[2, *] H. H. Chen,[2] and Y. K. Tsang[1, 2]
[1] Department of Electronic and Information Engineering
Hong Kong Polytechnic University
Hung Hom, Hong Kong SAR, P.R. China
[2] Department of Physics
University of Maryland
College Park, Maryland 20742

ABSTRACT: *A novel nondestructive technique is proposed to determine the longitudinal dispersion profile of an optical fiber which make uses of the output waveforms of the optical fiber from a set of input pulses and an optimization algorithm. The feasibility of the proposed method is demonstrated numerically.* © 2001 John Wiley & Sons, Inc. Microwave Opt Technol Lett 30: 312–314, 2001.

1. INTRODUCTION

The emergence of dispersion management as an important design tool in optical communication systems has led to the development of a number of nondestructive techniques to determine the variation of the chromatic dispersion parameter along a fiber span. Recently, two methods [1, 2] were developed to measure the zero dispersion point (ZDP) of an optical fiber based on the modulation-instability-induced gain at wavelengths longer than the ZDP, and on a search for the phase-matching condition in four-wave mixing. The dispersion at a given wavelength is then determined from the slope of the dispersion around the ZDP. The chromatic dispersion coefficients can also be measured directly based on the phase mismatch of four wave-mixing [3] or estimated from the observed distribution of mode-field diameter [4].

In this paper, we propose a new non-destructive technique to measure the dispersion distribution along a fiber. The proposed method is based on the observation that the output pulse shape from an optical fiber for an input pulse carries some information about the optical fiber that it passes through. The output waveforms depends on fiber characteristics such as dissipation, dispersion, self-phase modulation, Raman effect, etc., as well as the input pulse shapes. In general, different pulse shapes and amplitudes will carry different information about the fiber. Using an accurate model of light propagation in optical fibers, in principle, one can determine these fiber characteristics from the output waveforms. The situation is analogous to a scattering problem in which the scattering parameters are used to determine the structure of the scattering potential. In the following, we demonstrate that the proposed method can be used to determine the longitudinal dispersion profile of an optical fiber. Other fiber parameters such as the Kerr constant can be determined in a similar way.

The success of the proposed method depends on the choice of the theoretical model. The recent success of computer simulations in the study of light propagation in optical fibers underscores the fact that current theoretical models have captured the essential features of the propagation. For this study, we assume that light propagation in optical fibers is described by the modified nonlinear Schrödinger equation

$$i\frac{\partial q}{\partial z} + \frac{1}{2}f(z)\frac{\partial^2 q}{\partial t^2} + |q|^2 q = -i\Gamma q + i\beta\frac{\partial^3 q}{\partial t^3} \qquad (1)$$

where $q(z, t)$ is the slowly varying envelope of the electric field, z is the the normalized distance, t is normalized time, and Γ is the loss coefficient. The function $f(z)$ is the profile of the second-order dispersion coefficient, and β is the third-order dispersion coefficient. We assume that both Γ and β are unknown constants. The case in which the third-order dispersion coefficient is also a function of distance z can be treated in the same way as $f(z)$. It is possible to determine both the second- and third-order dispersion variation simultaneously with the proposed method. The output waveform $q(L, t)$ at a distance $z = L$ of an input pulse $q(0, t)$ depends on the dispersion profile $f(z)$ $(0 \leq z \leq L)$, the loss coefficient Γ, and the third-order dispersion coefficient β. In general, it is difficult, if not impossible, to invert $q(L, t)$ analytically to obtain $f(z)$, Γ, and β directly. Therefore, we formulate the inverse problem as an optimization problem as follows.

2. DESCRIPTION OF ALGORITHM

To simplify the following discussion, we assume for the moment that both Γ and β equal zero. The effects of loss and third-order dispersion will be included in the simulations. We assume that the longitudinal dispersion profile to be determined is given by $f_T(z)$. The output waveform at a distance $z = L$ of an input pulse shape $q(0, t)$ is given by $q_T(L, t)$. The output waveform for the same input pulse of a trial dispersion profile $f(z)$ using Eq. (1) is given by $q(L, t)$. We measure the deviation of $q(L, t)$ from the target output waveform $q_T(L, t)$ using error functions of the form $E_1 = \sum_{j=1}^{n} \int_{-\infty}^{+\infty} |q_j(L, t) - q_{jT}(L, t)|^2 \, dt$ or $E_2 = \sum_{j=1}^{n} \int_{-\infty}^{+\infty} [|q_j(L, t)|^2 - |q_{jT}(L, t)|^2]^2 \, dt$. The summation is done over a set of n different input pulses $q_j(0, t)$, $j = 1, \ldots, n$. The error function E_1 measures the amplitude and phase difference between $q_j(L, t)$ and $q_{jT}(L, t)$, while E_2 only measures the intensity difference between the two pulses. The essence of our method is to iteratively adjust the trial dispersion function $f(z)$ so that the error function E_1 or E_2 is minimized for a chosen set of input pulses. The trial dispersion profile will then approximate the dispersion profile of the fiber, provided that the theoretical model in Eq. (1) adequately describes light propagation in the fiber.

In the following, we assume that the dispersion profile is a continuous function of distance. The case in which there are discontinuous jumps in the dispersion $f(z)$, such as those found in the dispersion maps of some dispersion management systems, will be considered elsewhere. We can then expand the trial dispersion profile $f(z)$ as a finite Legendre series:

$$f(z) = \sum_{\mu=1}^{N} f_\mu \psi_\mu(z) \qquad (2)$$

where ψ_μ are Legendre polynomials of order μ, f_μ are the coefficients of the series expansion, and N is the order of truncation. The choice of truncation order will affect the accuracy of the determined dispersion profile and the computational time required. We measure the accuracy of the dispersion profiles using $\epsilon_f = \int_0^L dz |f(z) - f_T(z)|^2$. The inverse problem of determining the fiber dispersion profile from the output waveforms is now formulated as a minimization problem of the error function E_i with respect to the f_μ parameters. It is assumed that ϵ_f is minimized when E_i is minimized.

There are many ways to solve the minimization problem. We choose the conjugate gradient method [6] because of its robustness and efficiency. The gradient of the error function dE_i/df_μ, $i = 1$ or 2 is given by

$$\frac{dE_i}{df_\mu} = \sum_{j=1}^{n} \int_{-\infty}^{+\infty} \left(\frac{\delta E_i}{\delta q_j} \frac{\partial q_j}{\partial f_\mu} + \frac{\delta E_i}{\delta q_j^*} \frac{\partial q_j^*}{\partial f_\mu} \right) dt \qquad (3)$$

where $\delta E_i/\delta q_j$ and $\delta E_i/\delta q_j^*$ are the functional derivatives of the error function E_i with respect to q_j and q_j^*, respectively. The sensitivity functions $\partial q_j/\partial f_\mu$ and $\partial q_j^*/\partial f_\mu$ satisfy the linearized version of Eq. (1), i.e.,

$$i \frac{\partial \phi_{j,\mu}}{\partial z} + \frac{1}{2} f(z) \frac{\partial^2 \phi_{j,\mu}}{\partial t^2} + 2|q_j|^2 \phi_{j,\mu} + q_j^2 \phi_{j,\mu}^*$$
$$= -\frac{1}{2} \psi_\mu(z) \frac{\partial^2 q_j}{\partial t^2} \qquad (4)$$

where $\phi_{j,\mu}(z, t) = \partial q_j/\partial f_\mu$. Recall that Γ and β are assumed to be zero in this discussion. The functional derivatives $\delta E_i/\delta q_j$ and $\delta E_i/\delta q_j^*$ depend on the choice of the error function E_i, and can be determined from $q_j(L, t)$ and $q_{jT}(L, t)$ directly. For example,

$$\frac{\delta E_1}{\delta q_j} = q_j^*(L, t) - q_{jT}^*(L, t) \qquad (5)$$

and $\delta E_1/\delta q_j^*$ can be obtained by taking the complex conjugate of Eq. (5). Equations (1)–(5) constitute an optimization algorithm to determine $f_T(z)$. From an initial guess of the dispersion profile $f(z)$, we determine the output waveform $q_j(L, t)$ using Eq. (1). We then determine the sensitivity functions $\partial q_j/\partial f_\mu$ using Eq. (4). From Eq. (3), we calculate the gradient of the error function, and hence the corresponding change in the parameters f_μ using the conjugate-gradient algorithm [6]. The procedure is repeated until a given accuracy is reached.

3. NUMERICAL RESULTS

In practice, the target output waveforms $q_{jT}(L, t)$ are measured experimentally. However, in order to study the feasibility of the proposed method, we also used Eq. (1) with $f(z) = f_T(z)$ to generate $q_{jT}(L, t)$. Figure 1 shows the dispersion profiles determined from the optimization algorithm when $f_T(z)$ is a constant, a straight line, and an exponentially decreasing profile. Note that a log-linear plot is used; thus, the straight line in Figure 1 corresponds to an exponentially decreasing profile. The solid lines represent the target dispersion profiles in each of the three cases. The solid circles, solid squares, and crosses represent simulation results for $\Gamma = \beta = 0$. All simulated dispersion profiles in Figure 1 have $\epsilon_f < 10^{-5}$.

The dispersion profiles are determined with only one input pulse ($n = 1$) in all cases. The input pulse shape is Gaussian, with $q(0, t) = A\pi^{-1/4} \exp(-t^2/2)$. The initial amplitude A is chosen to be 1.5, and the pulse is propagated for a distance $L = 1$. We have used other input pulse shapes such as hyperbolic secant pulses. We found that simulations using Gaussian input pulses in general converge faster than those of the hyperbolic secant pulses. We have used a pulse amplitude A between 0.5 and 3. For the same pulse width, pulses with higher amplitudes are more sensitive to the variations in $f(z)$. In other words, for the same changes in
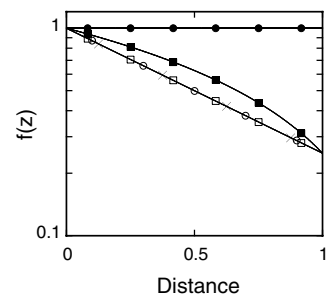

Figure 1 Simulated results for constant, straight line, and exponential decreasing dispersion profiles. The solid lines represent the targeted results. The solid circles, solid squares, and crosses are simulated results when $\Gamma = \beta = 0$. The open circles are results for $\Gamma = 0.69$ and $\beta = 0$. The open squares are results for $\Gamma = 0.69$ and $\beta = 1$

$f(z)$, stronger input pulses will produce larger changes in the output pulse $q(L, t)$ than those for weaker pulses. Thus, the values of the error function which measures the difference between the target waveform and the simulated waveform will be larger. For example, to determine $f(z)$ to an accuracy of $\epsilon_f = 10^{-5}$, E_2 can be as large as 10^{-1} for $A = 3$, while E_2 cannot be larger than 10^{-7} for $A = 0.5$. An error bound for E_2 of 10^{-7} in the pulse profiles is, of course, impractical. The situation is worse when fiber loss is taken into account because the effect of nonlinearity is weakened. A more stringent bound for E_2 is required for the same ϵ_f when compared to the lossless cases. For large amplitude pulses, depending on the initial guess of $f(z)$, the algorithm sometimes diverges or converges to a local minimum of the error function, i.e., the algorithm gives an incorrect answer for $f(z)$ even though the error function E_2 reaches the prescribed bound. Therefore, although our results indicate that a single input pulse is sufficient to determine the dispersion profile, a number of pulses arranged in order of increasing sensitivity is required to determine the dispersion profile correctly.

We had used both E_1 and E_2 as the error functions in determining the dispersion profile. The algorithm converges to the solution much faster when E_1 is used because both the amplitude and phase information of the output waveforms are included. The results depicted in Figure 1 are obtained using E_2, i.e., without the phase information in $q_{jT}(L, t)$. In all cases, the initial trial dispersion profile is chosen arbitrarily as $f(z) = 0.2$.

To include the effect of loss and third-order dispersion, Eqs. (3) and (4) are modified accordingly to take into account the variations with respect to the Γ and β parameters. The open circles in Figure 1 are simulated results for an exponentially decreasing profile with $\Gamma = 0.69$ and $\beta = 0$, and the open squares are simulated results with $\Gamma = 0.69$ and $\beta = 1$ for the same exponentially decreasing profile. At $\Gamma = 0.69$, the signal power will be reduced to $1/4$ of its initial value after propagation of a normalized distance $z = 1$. All other parameters are the same as the $\Gamma = 0$ and $\beta = 0$ case.

For the results presented in Figure 1, we use five Legendre polynomials ($N = 5$) to determine the profiles. The spatial resolution of the measurement can be improved by increasing the number of modes used in Eq. (2) at the expense of computational time. For example, we have the case where there are small sinusoidal noise components in an exponentially decreasing dispersion profile given by

$$f_T(z) = \exp(-\alpha z) + \delta[\sin(4\pi z) + \cos(4\pi z)] \quad (6)$$

where α is the rate of decrease of the dispersion profile and δ is the amplitude of the sinusoidal fluctuation. We choose $\alpha = 2\Gamma$ such that the exponentially decreasing dispersion matches the exponentially decreasing pulse power. For $\Gamma = 0.69$ and $\delta = 0.1$, the truncation error is 5×10^{-3} for $N = 5$ and 2×10^{-6} for $N = 10$. Figure 2 shows the simulated results for $N = 5$ and $N = 10$. The parameter $\beta = 0$. The solid line represents the targeted results. The dashed line and the dotted lines are results for $N = 5$ and $N = 10$, respectively. For $N = 5$, it takes 6000 CPU seconds for ϵ_f to reach an accuracy 6×10^{-3}, while for $N = 10$, it takes 9000 CPU seconds for ϵ_f to reach an accuracy 6×10^{-4}. The simulations were done on an ALPHAstation 500 workstation. We use 512 grid points for the t-direction and 1000 steps in the z-direction.

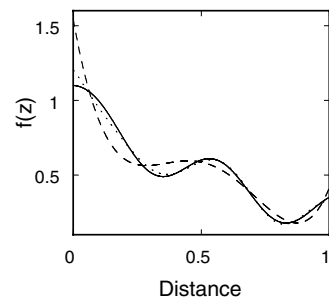In real units, the pulse width required for the measure-

Figure 2 Simulated results for exponentially decreasing dispersion profiles with sinusoidal noise components. The solid line represents the targeted results. The dashed line represents results using five Legendre modes, and the dotted line represents simulated results using ten Legendre modes. The parameters $\Gamma = 0.69$ and $\beta = 0$

ment is given by τ (ps) $= 1.13\sqrt{L/D}$, where L is the length of the fiber span in kilometers and D is the peak dispersion value in ps/nm $\cdot$ km. If $L = 50$ km and $D \approx 1$ ps/nm $\cdot$ km, the pulse width required is 8 ps. If the effective area of the fiber is 60 μm^2, the peak power of the input pulse will be 20 mW.

4. CONCLUSION

We demonstrate that it is possible to determine the fiber dispersion distribution using a theoretical model of light propagation in optical fibers and an optimization algorithm. The accuracy of the results depends on the validity of the fiber model used. The effects of timing jitter and amplitude jitter are not taken into account in Eq. (1), but because of the random nature of the jitters, Eq. (1) should adequately describe the average pulse evolution. The current model does not include polarization mode dispersion (PMD), which could become important for fibers with large PMD coefficients. The impact of PMD and noises in the output pulse forms on the accuracy of the determined dispersion profiles is under investigation. The formalism presented here can be generalized to determine other fiber parameters such as the longitudinal distribution of third-order dispersion coefficient or the Kerr constant.

REFERENCES

1. S. Nishi and M. Saruwatari, Technique for measuring the distributed zero dispersion wavelength of optical fibers using pulse amplification caused by modulation instability, Electron Lett 31 (1995), 225–226.
2. R.M. Jopson, M. Eiselt, R.H. Stolen, R.M. Derosier, A.M. Vengsarkar, and U. Koren, Non-destructive dispersion-zero measurements along an optical fiber, Electron Lett 31 (1995), 2115–2117.
3. L.F. Mollenauer, P.V. Mamyshev, and M.J. Neubelt, Method for facile and accurate measurement of optical fiber dispersion maps, Opt Lett 21 (1996), 1724–1726.
4. M. Ohashi and M. Tateda, Novel technique for measuring longitudinal chromatic dispersion distribution in single mode fibers, Electron Lett 29 (1993), 426–428.
5. A. Hasegawa and F. Tappert, Transmission of stationary nonlinear pulses in dispersive dielectric fibers. I. Anomalous dispersion. Appl Phys Lett 23 (1973), 142–144.
6. W.H. Press, B.P. Flannery, S.A. Teukolsky, and W.T. Vetterling, Numerical recipes in Fortran: The art of scientific computing, Cambridge University Press, Cambridge, England, 1992, p. 413.